PHYSICAL REVIEW D **81,** 031103(R) (2010)

Study of the $B \to X(3872)(\to D^{*0}\bar{D}^0)K$ decay

T. Aushev,[18,12] N. Zwahlen,[18] I. Adachi,[8] H. Aihara,[42] A. M. Bakich,[37] V. Balagura,[12] A. Bay,[18] K. Belous,[11] V. Bhardwaj,[33] M. Bischofberger,[24] A. Bondar,[1,31] A. Bozek,[28] J. Brodzicka,[28] T. E. Browder,[7] Y. Chao,[27] A. Chen,[25] P. Chen,[27] B. G. Cheon,[6] C.-C. Chiang,[27] R. Chistov,[12] I.-S. Cho,[46] S.-K. Choi,[5] Y. Choi,[36] J. Dalseno,[21,39] M. Danilov,[12] A. Drutskoy,[2] S. Eidelman,[1,31] N. Gabyshev,[1,31] P. Goldenzweig,[2] H. Ha,[16] J. Haba,[8] B.-Y. Han,[16] H. Hayashii,[24] Y. Hoshi,[41] W.-S. Hou,[27] H. J. Hyun,[17] T. Iijima,[23] K. Inami,[23] R. Itoh,[8] M. Iwabuchi,[46] M. Iwasaki,[42] Y. Iwasaki,[8] N. J. Joshi,[38] T. Julius,[22] D. H. Kah,[17] J. H. Kang,[46] P. Kapusta,[28] T. Kawasaki,[30] H. J. Kim,[17] H. O. Kim,[17] J. H. Kim,[36] Y. I. Kim,[17] Y. J. Kim,[4] B. R. Ko,[16] S. Korpar,[20,13] P. Križan,[19,13] P. Krokovny,[8] T. Kuhr,[15] R. Kumar,[33] Y.-J. Kwon,[46] J. S. Lange,[3] S.-H. Lee,[16] J. Li,[7] C. Liu,[34] D. Liventsev,[12] R. Louvot,[18] A. Matyja,[28] S. McOnie,[37] T. Medvedeva,[12] K. Miyabayashi,[24] H. Miyata,[30] Y. Miyazaki,[23] R. Mizuk,[12] E. Nakano,[32] M. Nakao,[8] Z. Natkaniec,[28] S. Nishida,[8] K. Nishimura,[7] O. Nitoh,[44] S. Ogawa,[40] T. Ohshima,[23] S. Okuno,[14] S. L. Olsen,[35,7] P. Pakhlov,[12] G. Pakhlova,[12] H. Palka,[28] C. W. Park,[36] H. Park,[17] H. K. Park,[17] R. Pestotnik,[13] M. Petrič,[13] L. E. Piilonen,[45] S. Ryu,[35] H. Sahoo,[7] K. Sakai,[30] Y. Sakai,[8] O. Schneider,[18] C. Schwanda,[10] K. Senyo,[23] M. Shapkin,[11] C. P. Shen,[7] J.-G. Shiu,[27] B. Shwartz,[1,31] J. B. Singh,[33] P. Smerkol,[13] A. Sokolov,[11] E. Solovieva,[12] M. Starič,[13] T. Sumiyoshi,[43] Y. Teramoto,[32] I. Tikhomirov,[12] K. Trabelsi,[8] S. Uehara,[8] T. Uglov,[12] Y. Unno,[6] S. Uno,[8] Y. Usov,[1,31] G. Varner,[7] K. Vervink,[18] C. H. Wang,[26] P. Wang,[9] Y. Watanabe,[14] R. Wedd,[22] J. Wicht,[8] E. Won,[16] B. D. Yabsley,[37] Y. Yamashita,[29] M. Yamauchi,[8] C. Z. Yuan,[9] Z. P. Zhang,[34] V. Zhulanov,[1,31] T. Zivko,[13] A. Zupanc,[13] and O. Zyukova[1,31]

(Belle Collaboration)

[1]*Budker Institute of Nuclear Physics, Novosibirsk*
[2]*University of Cincinnati, Cincinnati, Ohio 45221*
[3]*Justus-Liebig-Universität Gießen, Gießen*
[4]*The Graduate University for Advanced Studies, Hayama*
[5]*Gyeongsang National University, Chinju*
[6]*Hanyang University, Seoul*
[7]*University of Hawaii, Honolulu, Hawaii 96822*
[8]*High Energy Accelerator Research Organization (KEK), Tsukuba*
[9]*Institute of High Energy Physics, Chinese Academy of Sciences, Beijing*
[10]*Institute of High Energy Physics, Vienna*
[11]*Institute of High Energy Physics, Protvino*
[12]*Institute for Theoretical and Experimental Physics, Moscow*
[13]*J. Stefan Institute, Ljubljana*
[14]*Kanagawa University, Yokohama*
[15]*Institut für Experimentelle Kernphysik, Karlsruhe Institut für Technologie, Karlsruhe*
[16]*Korea University, Seoul*
[17]*Kyungpook National University, Taegu*
[18]*École Polytechnique Fédérale de Lausanne (EPFL), Lausanne*
[19]*Faculty of Mathematics and Physics, University of Ljubljana, Ljubljana*
[20]*University of Maribor, Maribor*
[21]*Max-Planck-Institut für Physik, München*
[22]*University of Melbourne, School of Physics, Victoria 3010*
[23]*Nagoya University, Nagoya*
[24]*Nara Women's University, Nara*
[25]*National Central University, Chung-li*
[26]*National United University, Miao Li*
[27]*Department of Physics, National Taiwan University, Taipei*
[28]*H. Niewodniczanski Institute of Nuclear Physics, Krakow*
[29]*Nippon Dental University, Niigata*
[30]*Niigata University, Niigata*
[31]*Novosibirsk State University, Novosibirsk*
[32]*Osaka City University, Osaka*
[33]*Panjab University, Chandigarh*
[34]*University of Science and Technology of China, Hefei*
[35]*Seoul National University, Seoul*
[36]*Sungkyunkwan University, Suwon*

[37]*School of Physics, University of Sydney, NSW 2006*
[38]*Tata Institute of Fundamental Research, Mumbai*
[39]*Excellence Cluster Universe, Technische Universität München, Garching*
[40]*Toho University, Funabashi*
[41]*Tohoku Gakuin University, Tagajo*
[42]*Department of Physics, University of Tokyo, Tokyo*
[43]*Tokyo Metropolitan University, Tokyo*
[44]*Tokyo University of Agriculture and Technology, Tokyo*
[45]*IPNAS, Virginia Polytechnic Institute and State University, Blacksburg, Virginia 24061*
[46]*Yonsei University, Seoul*

(Received 9 December 2009; published 22 February 2010)

We present a study of $B \to X(3872)K$ with $X(3872)$ decaying to $D^{*0}\bar{D}^0$ using a sample of 657×10^6 $B\bar{B}$ pairs recorded at the $\Upsilon(4S)$ resonance with the Belle detector at the KEKB asymmetric-energy e^+e^- collider. Both $D^{*0} \to D^0\gamma$ and $D^{*0} \to D^0\pi^0$ decay modes are used. We find a peak of $50.1^{+14.8}_{-11.1}$ events with a mass of $(3872.9^{+0.6+0.4}_{-0.4-0.5})$ MeV/c^2, a width of $(3.9^{+2.8+0.2}_{-1.4-1.1})$ MeV/c^2 and a product branching fraction $\mathcal{B}(B \to X(3872)K) \times \mathcal{B}(X(3872) \to D^{*0}\bar{D}^0) = (0.80 \pm 0.20 \pm 0.10) \times 10^{-4}$, where the first errors are statistical and the second ones are systematic. The significance of the signal is 6.4σ. The difference between the fitted mass and the $D^{*0}\bar{D}^0$ threshold is calculated to be $(1.1^{+0.6+0.1}_{-0.4-0.3})$ MeV/c^2. We also obtain an upper limit on the product of branching fractions $\mathcal{B}(B \to Y(3940)K) \times \mathcal{B}(Y(3940) \to D^{*0}\bar{D}^0)$ of 0.67×10^{-4} at 90% CL.

DOI: 10.1103/PhysRevD.81.031103 PACS numbers: 14.40.Rt, 12.39.Mk, 13.25.Hw

The $X(3872)$ was discovered by Belle in 2003 in $B^\pm \to J/\psi\pi^+\pi^-K^\pm$ [1] with a mass of $(3872.0 \pm 0.6 \pm 0.5)$ MeV/c^2, and was later confirmed by CDF [2], D0 [3] and *BABAR* [4]. It is one of the many new and unexpected hidden-charm states recently discovered with masses around 4 GeV/c^2. So far it remains unclassified; it does not seem to be a pure $c\bar{c}$ charmonium state, but may be a $D^*\bar{D}$ deuson [5,6], a tetraquark state [7] or a charmonium-gluon hybrid [8]. The current average mass in the $J/\psi\pi^+\pi^-$ channel is (3871.50 ± 0.19) MeV/c^2 [9].

An important feature of the $X(3872)$ is that its mass is very close to the $D^{*0}\bar{D}^0$ threshold $((3871.81 \pm 0.36)$ MeV/c^2 [13]). The $X(3872)$ was also observed by Belle [14] as a near-threshold enhancement in the $D^0\bar{D}^0\pi^0$ invariant mass spectrum of the $B \to D^0\bar{D}^0\pi^0K$ channel, with a peak at $(3875.2 \pm 0.7^{+0.3}_{-1.6} \pm 0.8)$ MeV/c^2, where the third error is from the uncertainty on the D^0 mass [13], a Gaussian width of (2.42 ± 0.55) MeV/c^2, and a branching fraction $\mathcal{B}(B \to D^0\bar{D}^0\pi^0K) = (1.22 \pm 0.31^{+0.23}_{-0.30}) \times 10^{-4}$. This initial study did not distinguish between decays via the D^{*0}, and more general $D^0\pi^0$ final states. Looking in addition for the $D^{*0} \to D^0\gamma$ decay is crucial to demonstrate the presence of $X(3872)$ decay through a D^{*0}.

The *BABAR* collaboration recently published an observation of the decay $B \to X(3872)(\to D^{*0}\bar{D}^0)K$ with a 4.9σ significance [15]. The observed mass is $(3875.1^{+0.7}_{-0.5} \pm 0.5)$ MeV/c^2 and the width is $(3.0^{+1.9}_{-1.4} \pm 0.9)$ MeV/c^2, with a product branching fraction $\mathcal{B}(B^+ \to X(3872)K^+) \times \mathcal{B}(X(3872) \to D^{*0}\bar{D}^0) = (1.67 \pm 0.36 \pm 0.47) \times 10^{-4}$. In the *BABAR* analysis, D^{*0} candidates were subjected to a mass-constrained fit.

Another new particle called $X(3940)$ was discovered by Belle in the $e^+e^- \to J/\psi D^*\bar{D}$ process [16]. A state with the same mass, the $Y(3940)$ (also known as $X(3945)$ [13]), was discovered by Belle in $B \to \omega J/\psi K$ [17] and was later confirmed by *BABAR*, albeit with a smaller mass [18]. The possibility that the $X(3940)$ and $Y(3940)$ are the same state has not yet been ruled out.

In this paper we study the decays of $X(3872)$ and $Y(3940)$ to $D^{*0}D^0$ final state, followed either by $D^{*0} \to D^0\gamma$ or $D^{*0} \to D^0\pi^0$, in the charged and neutral $B \to X(3872)K$ and $B \to Y(3940)K$ decays, respectively. Inclusion of charge-conjugate modes is implied throughout the paper. Furthermore, we use the notation $D^{*0}\bar{D}^0$ to indicate both $D^{*0}\bar{D}^0$ and $\bar{D}^{*0}D^0$. The results are based on a 605 fb^{-1} data sample, corresponding to $657 \times 10^6 B\bar{B}$ pairs, collected at the $\Upsilon(4S)$ resonance with the Belle detector [19] at the KEKB asymmetric-energy e^+e^- collider [20], which includes the statistics used in the previous Belle analysis [14].

The Belle detector is a general purpose spectrometer with a 1.5 T magnetic field provided by a superconducting solenoid. A silicon vertex detector and a 50-layer central drift chamber are used to measure the momenta of charged particles. Photons are detected in an electromagnetic calorimeter consisting of CsI(Tl) crystals. Particle identification likelihoods $\mathcal{L}_K$ and $\mathcal{L}_\pi$ are derived from information provided by an array of time-of-flight counters, an array of silica aerogel Cherenkov threshold counters and dE/dx measurements in the central drift chamber.

Charged tracks are identified as kaons using a requirement on the likelihood ratio $\mathcal{L}_K/(\mathcal{L}_K + \mathcal{L}_\pi)$, which has an efficiency of 88% for kaons and 10% for pions. Similarly, the charged pion selection has an efficiency of 98% for pions and 12% for kaons. π^0 candidates are reconstructed from pairs of photons with energies $E_\gamma > 50$ MeV and

with invariant mass in the range 118 MeV/$c^2 < M_{\gamma\gamma} <$ 150 MeV/c^2. A mass-constrained fit is applied to obtain the four-momenta of the π^0 candidates. K^0_S candidates are reconstructed in the $K^0_S \to \pi^+\pi^-$ mode with the requirement $|M_{\pi\pi} - m_{K^0_S}| < 15$ MeV/c^2, where $m_{K^0_S}$ is the K^0_S mass [13]. Requirements on the K^0_S vertex displacement from the interaction point and on the difference between vertex and K^0_S flight directions are applied. The K^0_S selection criteria are described in detail elsewhere [21]. A mass- and vertex-constrained fit is applied to improve the four-momenta measurements of the K^0_S candidates.

D^0 mesons are reconstructed in the modes $D^0 \to K^-\pi^+$, $K^-\pi^+\pi^0$, $K^-\pi^+\pi^+\pi^-$, $K^0_S\pi^+\pi^-$ and K^-K^+. The D^0 candidates are required to have a mass within ± 14 MeV/c^2 (± 26 MeV/c^2 for the $K^-\pi^+\pi^0$ mode) of the D^0 mass, 1864.8 MeV/c^2 [13]. This mass window width corresponds to $\pm 4\sigma$ ($\pm 3\sigma$ for $K^-\pi^+\pi^0$). Mass- and vertex-constrained fits are applied to improve the resolution of the four-momenta of D^0 candidates. D^0 candidates are combined with a photon or a π^0 to obtain D^{*0} candidates. The photon candidate is required to have an energy in excess of 100 MeV and shower shape variables that are consistent with an electromagnetic shower; the ratio of energy deposition in the central 3×3 and 5×5 crystals of the cluster is required to be greater than 0.8. A mass window of ± 27.5 MeV/c^2 for the $D^{*0} \to D^0\gamma$ channel and ± 6 MeV/c^2 for the $D^{*0} \to D^0\pi^0$ channel is applied ($\pm 3\sigma$), and a mass-constrained fit is used to improve the four-momenta of the D^{*0} candidates; the mass is constrained to 2007.0 MeV/c^2 [13].

B mesons are reconstructed by combining a $D^{*0}\bar{D}^0$ candidate with invariant mass $M_{D^*D} < 4.0$ GeV/c^2 and a charged or neutral kaon candidate. To further reduce the background, at least one $D^0(\bar{D}^0)$ is required to decay to $K^-\pi^+(K^+\pi^-)$. The beam-energy constrained mass $M_{\rm bc} = \sqrt{E^2_{\rm beam} - (\sum_i \vec{P}_i)^2}$, where $\vec{P}_i$ is the momentum of the ith daughter of the B candidate in the e^+e^- center-of-mass (CM) system, is required to be larger than 5.2 GeV/c^2. The energy difference $\Delta E = E_B - E_{\rm beam}$, where E_B is the CM energy of the B candidate and $E_{\rm beam}$ is the CM beam energy, is restricted to the range $|\Delta E| <$ 9 MeV for $D^{*0} \to D^0\gamma$ and $|\Delta E| < 12$ MeV for $D^{*0} \to D^0\pi^0$. Continuum $e^+e^- \to q\bar{q}$ background events ($q = u$, d, s, c) are suppressed by requiring the ratio of the second and zeroth Fox-Wolfram moments [22] to be smaller than 0.3.

The average B candidate multiplicity per event is 2.3 for $D^{*0} \to D^0\gamma$ and 2.7 for $D^{*0} \to D^0\pi^0$. We select the candidate with the smallest value of the quantity

$$\left(\frac{\Delta M_{D^0}}{\sigma_{M_{D^0}}}\right)^2 + \left(\frac{\Delta M_{\bar{D}^0}}{\sigma_{M_{D^0}}}\right)^2 + \left(\frac{\Delta(M_{D^{*0}} - M_{D^0})}{\sigma_{(M_{D^{*0}} - M_{D^0})}}\right)^2 + \left(\frac{\Delta E}{\sigma_{\Delta E}}\right)^2 \left[+ \left(\frac{\Delta M_{\pi^0}}{\sigma_{M_{\pi^0}}}\right)^2 \right], \quad (1)$$

where Δx is the deviation of the measured quantity x from its expected value and σ_x the uncertainty in its measurement obtained using a Monte Carlo (MC) method, and the last term applies to the $D^{*0} \to D^0\pi^0$ channel only.

MC samples are produced using the EVTGEN [23] generator. The $X(3872)$ mass distribution is generated according to a relativistic Breit-Wigner function

$$BW(m) = \frac{\mu m \Gamma(m)}{(m^2 - \mu^2)^2 + \mu^2\Gamma(m)^2}, \quad (2)$$

where

$$\Gamma(m) = \Gamma_0 \frac{\mu}{m} \frac{p(m)}{p(\mu)},$$

$$p(m) = \frac{1}{2m} \times \sqrt{(m^2 - (m_{D^0} + m_{D^{*0}})^2)}\sqrt{(m^2 - (m_{D^0} - m_{D^{*0}})^2)},$$

and μ and Γ_0 are the nominal mass and width of the resonance, respectively, and $p(m)$ is the momentum of one of the daughters in the rest frame of its parent. The term $m\Gamma(m)$ in the numerator of Eq. (2) behaves like a phase-space function, giving a smooth rise near the $D^{*0}\bar{D}^0$ threshold.

The response of the Belle detector is simulated using a GEANT3-based program [24]. Since the $X(3872)$ is very close to the $D^{*0}\bar{D}^0$ threshold, its mass resolution varies rapidly with the $D^{*0}\bar{D}^0$ mass ($M_{D^*\bar{D}}$). This resolution was studied in detail using MC simulations. It is modeled as a single Gaussian with a width given by the function $a\sqrt{M_{D^*D} - m_0}$ (where a and m_0 are free parameters) shown in Fig. 1. At 3872 MeV/c^2, the resolution is 0.13 MeV/c^2.

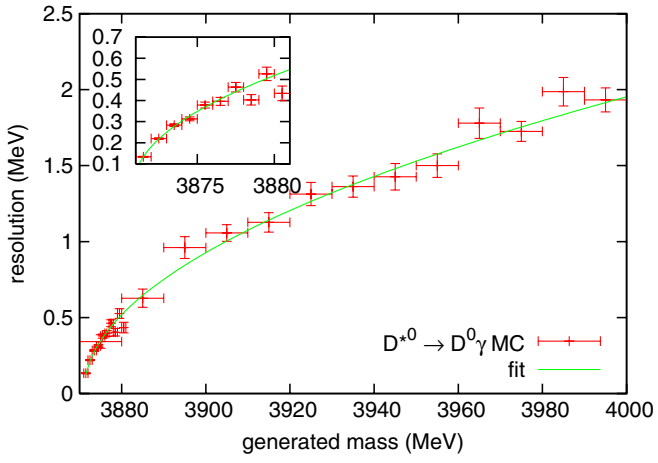

FIG. 1 (color online). $X(3872)$ mass resolution as a function of the $X(3872)$ mass in the $D^0\gamma$ channel, obtained from MC with a $X(3872)$ mass spectrum generated for a continuous range of masses from threshold to 4.0 GeV/c^2. Crosses are Gaussian resolutions for various generated $D^{*0}\bar{D}^0$ masses; the curve is the result of a fit with a square root function. Very similar results are obtained for the $D^0\pi^0$ channel.

A two-dimensional unbinned extended maximum likelihood fit to $M_{\rm bc}$ and M_{D^*D} is performed. The $M_{\rm bc}$ distribution is described by a single Gaussian function for the signal and an ARGUS function [25] for the background; the M_{D^*D} distribution is described by a relativistic Breit-Wigner function convoluted with the mass-dependent Gaussian resolution for the signal and a square root function for the background. In the $D^0\gamma$ channel, the signal function also includes a broad higher mass distribution, corresponding to $D^{*0}(D^0\gamma)\bar{D}^0$ events incorrectly reconstructed as $D^0\bar{D}^{*0}(\gamma\bar{D}^0)$. The shape and fraction of this contribution is determined from MC. In the $D^0\pi^0$ channel, however, the reflection shape is too similar to the signal one to be distinguished. This is taken into account as a systematic uncertainty. Additional components are the $Y(3940)$ signal, described by a relativistic Breit-Wigner function, and the nonresonant $B \to D^*\bar{D}K$ background, which peaks in $M_{\rm bc}$ but not in M_{D^*D} and is therefore described by a single Gaussian function in $M_{\rm bc}$ and a square root function in M_{D^*D}. The fitting procedure has been extensively tested using toy MC samples.

First, each D^{*0} decay channel sample is fitted separately. The yield, mass and width of the $X(3872)$ peak are free parameters of the fit, as well as the $Y(3940)$ yield and the number of background and nonresonant $B \to D^*\bar{D}K$ events. The $Y(3940)$ mass and its width are fixed to the values of Ref. [17]. The results of the fits are presented in Table I. Since all the results are consistent we proceed with a combined fit.

We subsequently perform a simultaneous fit to both D^{*0} modes where the mass and width of the signal function are constrained to have the same values in both modes, but the ratio of the yields in the $D^0\gamma$ and $D^0\pi^0$ channels is left free. Table I shows the fit results. We obtain a yield ratio of $N_{D^0\gamma}/N_{D^0\pi^0} = 1.16^{+0.53}_{-0.37}$, which is consistent with the value of 0.92 we expect from MC with no nonresonant $D^0\bar{D}^0\pi^0$ contribution. We then fix the ratios of $D^0\gamma/D^0\pi^0$ signal yields for the $X(3872)$ and $Y(3940)$ from MC studies assuming that the $D^0\pi^0$ and $D^0\gamma$ come from a D^{*0}. This fit gives $50.1^{+14.8}_{-11.1}$ events with a statistical significance of 7.9σ (see Fig. 2 and Table I). We compute the significance from $-2\ln(\mathcal{L}_0/\mathcal{L}_{\rm max})$, where $\mathcal{L}_0$ and $\mathcal{L}_{\rm max}$ are the likelihood values returned by the fit with the signal yield fixed at zero and left free, respectively. This quantity should be distributed as $\chi^2(n_{\rm dof} = 3)$, as three parameters are free for the signal. The results of the simultaneous fits are consistent with the results of the individual fits. The distributions for $M_{\rm bc}$ and $X(3872)$ mass closer to the $X(3872)$ signal region are presented in Fig. 3.

TABLE I. Summary of results: the fitted mass, width, and yield of the $X(3872)$ peak, and the total reconstruction efficiency, branching fraction and statistical significance for the various fits described in the text.

Sample	M_X (MeV/c^2)	Γ (MeV/c^2)	Yield	$\epsilon \times \mathcal{B}$	$\mathcal{B}$ (10^{-4})	σ
$D^{*0} \to D^0\gamma$ (XK^+ and XK^0)	3873.4 ± 1.0	$4.2^{+3.7}_{-1.8}$	$26.2^{+9.0}_{-7.6}$	4.56×10^{-4}	$0.87 \pm 0.28 \pm 0.10$	4.4σ
$D^{*0} \to D^0\pi^0$ (XK^+ and XK^0)	3872.8 ± 0.7	$3.1^{+4.1}_{-1.5}$	$22.0^{+10.7}_{-6.4}$	4.93×10^{-4}	$0.68 \pm 0.26 \pm 0.09$	6.8σ
All (free $D^0\gamma/D^0\pi^0$ ratio)	$3872.9^{+0.6}_{-0.4}$	$3.9^{+2.7}_{-1.4}$	$50.6^{+14.2}_{-11.0}$	9.49×10^{-4}	$0.81 \pm 0.20 \pm 0.10$	7.9σ
All (fixed $D^0\gamma/D^0\pi^0$ ratio)	$3872.9^{+0.6}_{-0.4}$	$3.9^{+2.8}_{-1.4}$	$50.1^{+14.8}_{-11.1}$	9.49×10^{-4}	$0.80 \pm 0.20 \pm 0.10$	7.9σ
$B^+ \to XK^+$	3872.9 (fixed)	3.9 (fixed)	$41.3^{+9.1}_{-8.1}$	8.17×10^{-4}	$0.77 \pm 0.16 \pm 0.10$	7.6σ
$B^0 \to XK^0$	3872.9 (fixed)	3.9 (fixed)	$8.4^{+4.5}_{-3.6}$	1.32×10^{-4}	$0.97 \pm 0.46 \pm 0.13$	2.8σ

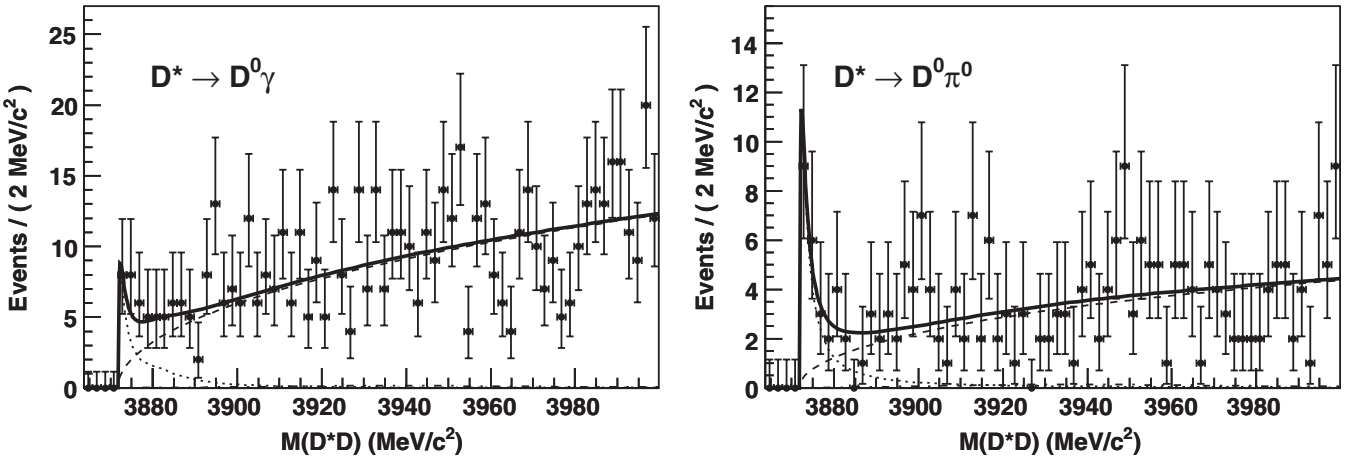

FIG. 2. Distributions of M_{D^*D} mass for $M_{\rm bc} > 5.27$ GeV/c^2 for $D^{*0} \to D^0\gamma$ (left) and for $D^{*0} \to D^0\pi^0$ (right). The result of the simultaneous fit is shown by the superimposed lines. The points with error bars are data, the dotted curve is the signal, the dashed curve is the background, the dash-dotted curve (barely visible) is the $Y(3940)$ component, and the solid curve is the total fitting function.

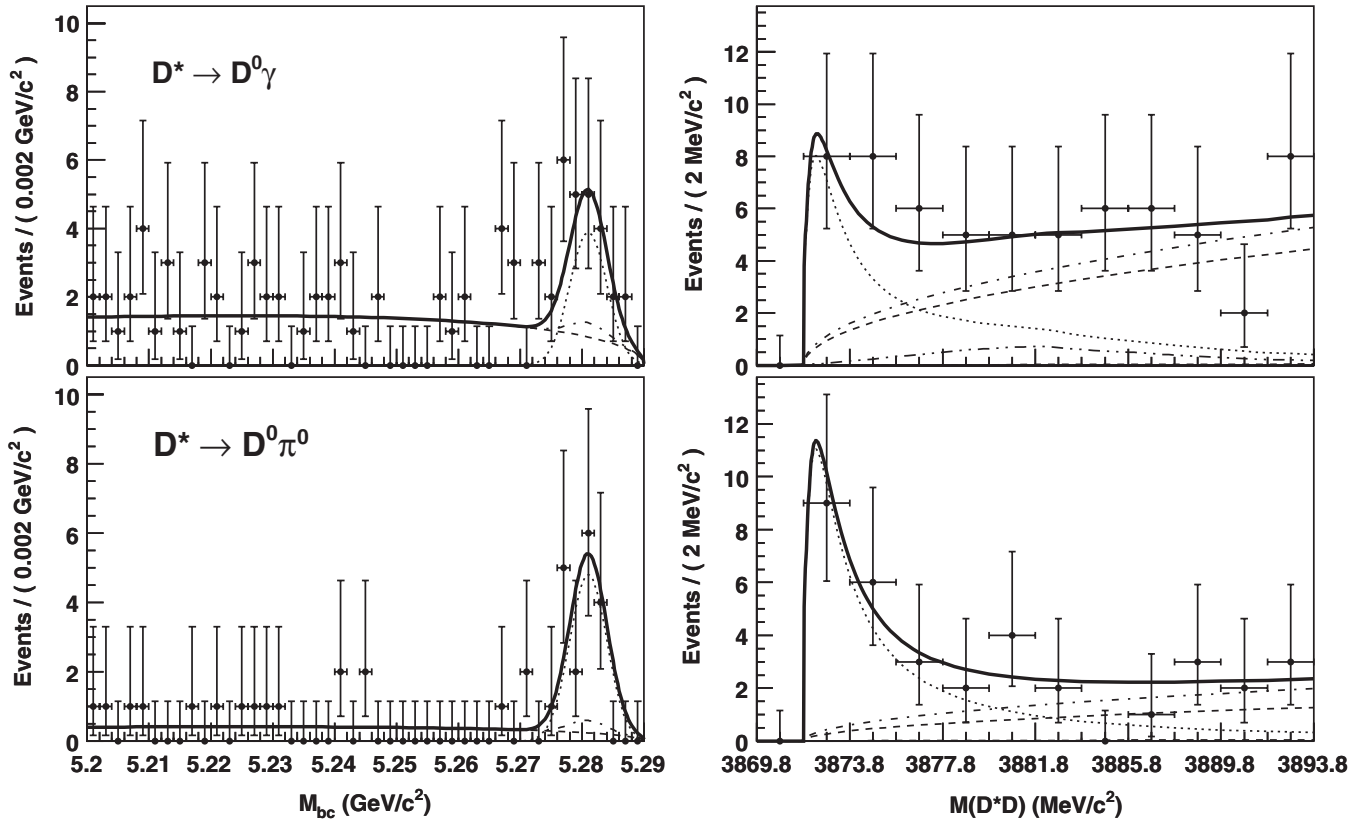

FIG. 3. Distributions of $M_{\rm bc}$ for $M_{D^*D} < 3.88$ GeV$/c^2$ (left) and of M_{D^*D} for $M_{\rm bc} > 5.27$ GeV$/c^2$ (right); the top row is for $D^{*0} \to D^0\gamma$ and the bottom row for $D^{*0} \to D^0\pi^0$. The result of the simultaneous fit is shown by the superimposed lines. The points with error bars are data, the dotted curve is the signal, the dashed curve is the background, the dash-dotted curve is the sum of the background and the $B \to D^*DK$ component, the dot-dot-dashed curve is the contribution from $D^0 - \bar{D}^0$ reflections, and the solid curve is the total fitting function.

Next we fit the $B^+ \to X(3872)K^+$ and $B^0 \to X(3872)K^0_S$ modes separately, fixing the $X(3872)$ mass and width to the values obtained with the simultaneous fit. Table I shows the results of these fits. Assuming the $B^0 \to X(3872)K^0$ transition rate to be equal to twice the $B^0 \to X(3872)K^0_S$ rate, we obtain a ratio of branching fractions

$$\frac{\mathcal{B}(B^0 \to X(3872)K^0)}{\mathcal{B}(B^+ \to X(3872)K^+)} = 1.26 \pm 0.65 \pm 0.06,$$

which is consistent with unity. In this ratio, most of the systematic uncertainties cancel out. The remaining uncertainties are MC statistics, particle identification and reconstruction efficiencies of the K^+ and K^0_S, which combine in quadrature to a 5% uncertainty.

The systematic uncertainties for the mass, width and signal yield are estimated by varying the fixed parameters of the simultaneous fit: the resolution function is scaled by factors 0.9 and 1.2 obtained from the inclusive D^{*0} mass resolution study; the ratio between $D^0\gamma$ and $D^0\pi^0$ yields is varied according to the error in the relative branching ratio between $D^{*0} \to D^0\gamma$ and $D^{*0} \to D^0\pi^0$ [13] and the uncertainty in their relative reconstruction efficiency; the $Y(3940)$ mass and width are fixed instead to the values from Ref. [18]; the yield of $Y(3940)$ is fixed to zero and to the upper limit of 40 events; the shape of the combinatorial background is changed from a square root to an inverted ARGUS function. Additional uncertainties due to possible biases of the fit parameters are obtained using a large ensemble of toy MC experiments generated for different values of $X(3872)$ mass and width. We also consider systematic uncertainties due to the contribution from $D^{*0}\bar{D}^0 \to D^0\bar{D}^{*0}$ misreconstruction by changing the shape of the miss-reconstruction component to one obtained from MC generated with different values of $X(3872)$ mass and width. Using MC we verify that the cross feeds between $D^0\bar{D}^0\gamma$ and $D^0\bar{D}^0\pi^0$ do not produce peaks in the signal region. Another systematic uncertainty on the mass is due to the $D^{*0}\bar{D}^0$ threshold mass, $2m_{D^0} + \Delta(m_{D^{*0}} - m_{D^0}) = (3871.80 \pm 0.41)$ MeV$/c^2$ [13]. The systematic uncertainties for the branching fraction are estimated from the following sources: the number of $B\bar{B}$ events, D^0 branching fractions, track finding efficiencies, K/π identification efficiency, γ or π^0 detection efficiency, K^0_S reconstruction efficiency, limited MC statistics and variation of the fixed parameters of the fit. Table II summarizes the systematic uncertainties. We obtain total systematic errors of

TABLE II. Sources of systematic uncertainties for the fitted mass and width (MeV/c^2) and for the $B \to X(3872)K$ branching fraction (%).

Source	Mass	Width	$\mathcal{B}$
Resolution function	± 0.04	± 0.09	± 0.3
$D^0\gamma/D^0\pi^0$ yields ratio	± 0.01	± 0.00	± 0.2
$Y(3940)$ parameters	± 0.01	$^{+0.00}_{-0.32}$	$^{+0.0}_{-4.0}$
Background shape	± 0.00	$^{+0.00}_{-0.14}$	$^{+0.0}_{-2.2}$
Fit bias	$^{+0.05}_{-0.30}$	$^{+0.15}_{-1.00}$	$^{+5.0}_{-0.0}$
$D^0 - \bar{D}^0$ reflections	± 0.02	± 0.11	± 0.5
D^0 and D^{*0} masses	± 0.41	–	–
Number of $B\bar{B}$ events	–	–	± 1.4
D^0 branching fractions	–	–	± 2.4
Tracking efficiency	–	–	± 5.0
Particle identification	–	–	± 4.0
γ or π^0 reconstruction	–	–	± 7.3
K^0_S reconstruction	–	–	± 4.5
MC statistics (efficiency)	–	–	± 1.4
Total (quadrature)	$^{+0.41}_{-0.54}$	$^{+0.22}_{-1.07}$	± 12

$^{+0.41}_{-0.54}$ MeV/c^2 for the mass, $^{+0.22}_{-1.07}$ MeV/c^2 for the width and $\pm 12\%$ for the branching fraction measurement. The significance of the signal including systematic uncertainties decreases to 6.4σ.

In order to determine the reconstruction efficiency for the branching fraction measurement, MC samples of $B^+ \to X(3872)(\to D^{*0}\bar{D}^0)K^+$ and $B^0 \to X(3872) \times (\to D^{*0}\bar{D}^0)K^0_S$ events are generated for $D^{*0} \to D^0\gamma$ and for $D^{*0} \to D^0\pi^0$. The $X(3872)$ is generated with a mass of 3872.5 MeV/c^2 and a width of 4.0 MeV/c^2. The total MC efficiencies multiplied by subdecay branching fractions are presented in Table I.

The branching fraction, assumed to be equal for charged and neutral B modes, is

$$\mathcal{B}(B \to X(3872)K) \times \mathcal{B}(X(3872) \to D^{*0}\bar{D}^0) = (0.80 \pm 0.20 \pm 0.10) \times 10^{-4}, \quad (3)$$

where $\mathcal{B}(X(3872) \to D^{*0}\bar{D}^0)$ stands for the sum of branching fractions for $X(3872) \to D^{*0}\bar{D}^0$ and $X(3872) \to \bar{D}^{*0}D^0$.

We obtain a mass of $(3872.9^{+0.6+0.4}_{-0.4-0.5})$ MeV/c^2 and a width of $(3.9^{+2.8+0.2}_{-1.4-1.1})$ MeV/c^2. The difference in mass between the peak and the $D^{*0}\bar{D}^0$ threshold is

$$\delta M = M_X - m_{D^{*0}} - m_{D^0} = (1.1^{+0.6+0.1}_{-0.4-0.3}) \text{ MeV}/c^2. \quad (4)$$

As a cross-check, different shapes are used as a signal function to fit the data. Using a nonrelativistic Breit-Wigner function truncated at the threshold, we obtain a mass of $(3873.4^{+0.6}_{-0.9})$ MeV/c^2, a width of $(4.3^{+2.5}_{-1.4})$ MeV/c^2 and a signal yield of $39.6^{+9.3}_{-8.1}$ events with a statistical significance of 8.0σ. Using a Flatté-like parametrization [26], with $g = 0.3$ and $f_\rho = 0.007$, we obtain $E_f = (-14.9 \pm 2.0)$ MeV/c^2, consistent with expected $E_f = -11$ MeV/c^2 [26], and a signal of 65 ± 12 events with a statistical significance of 8.8σ. The data statistics are not sufficient to distinguish between other fitting functions suggested in the literature [27].

The peak mass in this mode, M_X, like that in the *BABAR* analysis [15], should not be directly compared to the mass of the peak seen in $J/\psi\pi^+\pi^-$, or to the mass of the $X(3872)$ state itself. In this analysis, to improve signal/background separation, $D^0\gamma$ and $D^0\pi^0$ combinations are each subjected to a mass window selection, and then a mass-constrained fit. This procedure returns masses above $D^{*0}\bar{D}^0$ threshold by construction, so the distribution (and the mass and width of the peak) should be interpreted accordingly. Efforts in this direction have already appeared in the literature [27,28], addressing a preliminary version of the results in this paper. It should be noted that the mass measurement in our earlier paper [14], while lacking the mass constraint, is also nontrivial to interpret, due to the role of the D^* width, and interference, in the decay amplitudes [27,28].

For the $Y(3940)$ state, the simultaneous fit yields $7 \pm 21 \pm 4$ signal events and we set an upper limit of

$$\mathcal{B}(B \to Y(3940)K) \times \mathcal{B}(Y(3940) \to D^{*0}\bar{D}^0) < 0.67 \times 10^{-4} \quad (5)$$

at 90% CL. By averaging the branching fractions of Refs. [17,18], we obtain $\mathcal{B}(B \to Y(3940)K) \times \mathcal{B}(Y(3940) \to \omega J/\psi) = (0.51 \pm 0.11) \times 10^{-4}$; combining this with the upper limit (5) we get $\frac{\mathcal{B}(Y(3940)\to\omega J/\psi)}{\mathcal{B}(Y(3940)\to D^{*0}\bar{D}^0)} > 0.71$ at 90% CL, to be compared with the 90% CL limits from Ref. [16], $\mathcal{B}(X(3940) \to \omega J/\psi) < 0.26$ and $\mathcal{B}(X(3940) \to D^{*0}\bar{D}^0) > 0.45$, thus $\frac{\mathcal{B}(X(3940)\to\omega J/\psi)}{\mathcal{B}(X(3940)\to D^{*0}\bar{D}^0)} < 0.58$ with more than 90% CL, an incompatibility that suggests that the $X(3940)$ and the $Y(3940)$ are different states.

In summary, we find a significant near-threshold enhancement in the $D^{*0}\bar{D}^0$ invariant mass spectrum in $B \to D^{*0}\bar{D}^0K$ decays. The significance of this enhancement including systematic uncertainties is 6.4σ; significant signals are seen in both $D^{*0} \to D^0\gamma$ and $D^0\pi^0$ modes. Using a relativistic Breit-Wigner, we obtain a mass of $(3872.9^{+0.6+0.4}_{-0.4-0.5})$ MeV/c^2 and a width of $(3.9^{+2.8+0.2}_{-1.4-1.1})$MeV/$c^2$. The difference between the fitted mass and the $D^{*0}\bar{D}^0$ threshold is $(1.1^{+0.6+0.1}_{-0.4-0.3})$ MeV/c^2. Note that a D^{*0} mass constraint has been used in this analysis; the fitted mass of the $X(3872)$ peak is 2.3σ lower than the value obtained by *BABAR* [15], where a similar constraint was used. For the $Y(3940)$ state, we set an upper limit on the $\mathcal{B}(B \to Y(3940)K) \times \mathcal{B}(Y(3940) \to D^{*0}\bar{D}^0)$ branching fraction which suggests that the $X(3940)$ and the $Y(3940)$ are different states.

We thank the KEKB group for the excellent operation of the accelerator, the KEK cryogenics group for the efficient

solenoid operations, and the KEK computer group and the NII for valuable computing and SINET3 network support. We acknowledge support from MEXT, JSPS and Nagoya's TLPRC (Japan), ARC and DIISR (Australia), NSFC (China), MSMT (Czechia), DST (India), MEST, NRF, NSDC of KISTI (Korea), MNiSW (Poland), MES and RFAAE (Russia), ARRS (Slovenia), SNSF (Switzerland), NSC and MOE (Taiwan), and DOE (USA).

[1] S.-K. Choi *et al.* (Belle Collaboration), Phys. Rev. Lett. **91**, 262001 (2003).
[2] D. Acosta *et al.* (CDF Collaboration), Phys. Rev. Lett. **93**, 072001 (2004).
[3] V. M. Abazov *et al.* (D0 Collaboration), Phys. Rev. Lett. **93**, 162002 (2004).
[4] B. Aubert *et al.* (*BABAR* Collaboration), Phys. Rev. D **71**, 071103 (2005).
[5] E. S. Swanson, Phys. Lett. B **588**, 189 (2004).
[6] N. A. Törnqvist, Phys. Lett. B **590**, 209 (2004).
[7] L. Maiani, F. Piccinini, A. D. Polosa, and V. Riquer, Phys. Rev. D **71**, 014028 (2005).
[8] B. A. Li, Phys. Lett. B **605**, 306 (2005).
[9] Our own average using the most recent measurements from Belle, *BABAR*, CDF and D0 [3,10–12].
[10] I. Adachi *et al.* (Belle Collaboration), arXiv:0809.1224.
[11] B. Aubert *et al.* (*BABAR* Collaboration), Phys. Rev. D **77**, 111101 (2008).
[12] T. Aaltonen *et al.* (CDF Collaboration), Phys. Rev. Lett. **103**, 152001 (2009).
[13] C. Amsler *et al.* (Particle Data Group), Phys. Lett. B **667**, 1 (2008).
[14] G. Gokhroo *et al.* (Belle Collaboration), Phys. Rev. Lett. **97**, 162002 (2006).
[15] B. Aubert *et al.* (*BABAR* Collaboration), Phys. Rev. D **77**, 011102 (2008).
[16] P. Pakhlov *et al.* (Belle Collaboration), Phys. Rev. Lett. **98**, 082001 (2007).
[17] S.-K. Choi, S. L. Olsen *et al.* (Belle Collaboration), Phys. Rev. Lett. **94**, 182002 (2005).
[18] B. Aubert *et al.* (*BABAR* Collaboration), Phys. Rev. Lett. **101**, 082001 (2008).
[19] A. Abashian *et al.* (Belle Collaboration), Nucl. Instrum. Methods Phys. Res., Sect. A **479**, 117 (2002).
[20] S. Kurokawa and E. Kikutani, Nucl. Instrum. Methods Phys. Res., Sect. A **499**, 1 (2003).
[21] F. Fang, Ph.D. thesis, University of Hawaii, 2003.
[22] G. C. Fox and S. Wolfram, Phys. Rev. Lett. **41**, 1581 (1978).
[23] D. J. Lange, Nucl. Instrum. Methods Phys. Res., Sect. A **462**, 152 (2001).
[24] R. Brun *et al.*, CERN Report DD/EE/84-1, 1984.
[25] H. Albrecht *et al.* (ARGUS Collaboration), Phys. Lett. B **185**, 218 (1987).
[26] C. Hanhart, Yu. S. Kalashnikova, A. E. Kudryavtsev, and A. V. Nefediev, Phys. Rev. D **76**, 034007 (2007).
[27] E. Braaten and J. Stapleton, Phys. Rev. D **81**, 014019 (2010).
[28] Yu. S. Kalashnikova and A. V. Nefediev, Phys. Rev. D **80**, 074004 (2009).